ELSEVIER

Coordination Chemistry Reviews
148 (1996) 71–96

COORDINATION CHEMISTRY REVIEWS

Synthesis and metallophilic properties of troponoid thiocrown ethers

Akira Mori [a], Kanji Kubo [b], Hitoshi Takeshita [a,*]

[a] *Institute of Advanced Material Study, 86, Kyushu University, Kasuga-koen, Kasuga, Fukuoka 816, Japan*
[b] *Graduate School of Engineering Sciences, 39, Kyushu University, Kasuga-koen, Kasuga, Fukuoka 816, Japan*

Received 27 January 1995

Contents

Abstract . . . 71
1. Introduction . . . 72
2. Preparation of troponoid dithiocrown ethers . . . 73
   2.1. From 5-hydroxytropolone (**1**) . . . 73
   2.2. From hinokitiol . . . 76
   2.3. From tropones . . . 76
3. Complex formation . . . 78
   3.1. 4,7-Disubstituted troponoid dithiocrown ethers **6** . . . 78
   3.2. 3,7-Disubstituted troponoid dithiocrown ethers **11d** and **11e** . . . 80
   3.3. 2,7-Disubstituted troponoid dithiocrown ethers **20** and **23** . . . 80
   3.4. 2,7-Disubstituted troponoid dithiocrown ethers **20**, **21c,d** and **26** and 4,7-disubstituted troponoid dithiocrown ethers **30** with thiocyanates . . . 82
4. Transport . . . 83
5. Association constant . . . 89
   5.1. UV spectrometry . . . 89
   5.2. ^{1}H NMR spectrometry . . . 92
6. Stereostructure of the mercurophilic dithiocrown derivative . . . 94
7. Conclusions . . . 95
References . . . 95

Abstract

A new class of ionophores with troponoid and thiocrown ether units was prepared. Cation-binding properties of troponoid dithiocrown ethers were characterized using UV and NMR spectroscopies. They have affinity with metal ions; in particular, they showed high affinity with Hg^{2+}. Transport of Hg^{2+} through a $CHCl_3$ liquid membrane with troponoid dithiocrown

*Corresponding author.

0010-8545/96/$32.00 © 1996 Elsevier Science S.A. All rights reserved
SSDI 0010-8545(95)01174-9

ethers was examined in a U-type cell. From an aqueous solution of $HgCl_2$ and $CuCl_2$, Hg^{2+} is transferred selectively and smoothly, while the Cu^{2+} remained quantitatively in the original solution. The cavity size of dithiocrown ethers is one of the requirements for effective extraction and transport of Hg^{2+}. However, derivatives with a smaller cavity still extract and transport Hg^{2+}. A polymer-supported troponoid dithiocrown ether was prepared to transport Hg^{2+} effectively and repeatedly. Comparing the troponoid dithiocrown ether with the benzenoid dithiocrown ether with a similar cavity size, the former was more effective for the transport of Hg^{2+}. It is proposed that the tropone ring assisted the release of Hg^{2+} from the complex by Coulomb repulsion between the protonated tropone ring and Hg^{2+}.

Keywords: Ionophores; Troponoid thiocrown ethers

1. Introduction

Crown ethers have played an important role in host–guest chemistry since the discovery of the formation of their complexes with various metal ions [1,2]. At the same time, considerable attention has been devoted to the development of new ionophores to achieve selective complexation of metal ions; the design of these highly selective ionophores is of great importance with respect to the effective separation and recovery of metal ions. In particular, metal ions such as Hg^{2+} and Cd^{2+} which are harmful to ecosystems should be removed and recovered efficiently.

2-Hydroxy-2,4,6-cycloheptatrien-1-ones (tropolones) enols of a cyclic α-diketone form complexes with metal ions [3–5]. It is known that hinokitiol exists in the heartwood of a conifer, *Chamaecyparis taiwanesis*, both as a free form and as an iron complex, called hinokitin, which is soluble in organic solvents [6]. However, few systematic studies of the application of this unique affinity towards metal ions of troponoids have been carried out. Asao and Kikuchi [7] observed that 2,4,6-cycloheptatrien-1-one (tropone) and 2-methoxytropone also formed complexes with metal ions; tropone formed a complex with $HgCl_2$, a 2:1 complex with $ZnCl_2$, and 1:1 complexes with $CdCl_2$, $CoCl_2$, $MnCl_2$, or $NiCl_2$, indicating that the free hydroxyl group of tropolones is not necessary for complexation. Tropones are easily

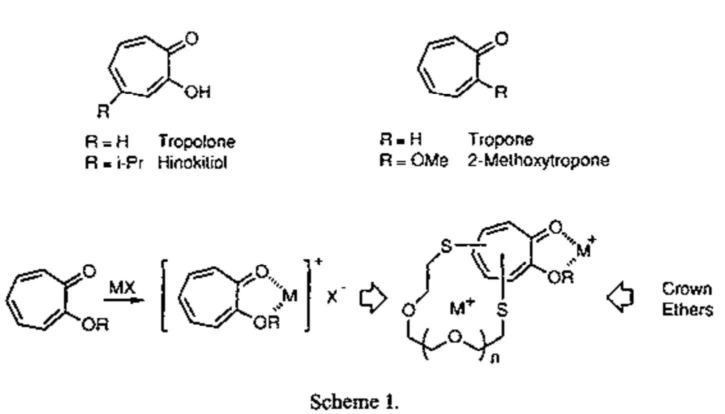

Scheme 1.

liberated from their complexes by hydrolysis, chromatography on SiO_2, or treatment with dioxane [7]. Thiocrown ethers [8–13] show high affinity toward soft, heavy metal ions such as Ag^+, Hg^{2+}, and Cd^{2+}, but they have no affinity towards hard metal such as like K^+ and Na^+.

Based on these observations, we are interested in the host–guest chemistry of the crown ethers with a troponoid unit, which have two complexing sites. The unique affinities for metal ions of troponoids and crown ethers would cooperate to construct a new class of readily synthesizable ionophores. Here, we demonstrate the synthesis and some physico-chemical properties of Hg^{2+}-capturing dithiocrown ethers of troponoids.

2. Preparation of troponoid dithiocrown ethers

2.1. From 5-hydroxytropolone (1)

It has been recognized [14] that the introduction of alkyl substituents at troponoid nuclei is limited since electrophilic substitution reactions of troponoids were inhibited under acidic conditions because of the formation of a tropylium cation. Previously, we have found that 4,6-bis(chloromethyl)-2,5-dimethoxytropone (2) [15] was formed from ethyl chloroformate and 4,6-bis(morpholinomethyl)-2,5-dimethoxytropone (3) [16], which was prepared from the Mannich reaction between 1 and a mixture of morpholine and formaldehyde followed by methylation with diazomethane.

When a MeOH solution of 2 reacts with oligoethylene glycol bis(mercaptoethyl) ethers **4a–e**, two types of macrocyclic dithiocrown ethers **5a,b** or **6c–e** are formed, respectively [17,18]. In the reaction of 2 with bis(mercaptoethyl) ether (**4b**), the product is **5b**. The structure of **5b** was deduced from NMR spectral analysis, which showed two proton signals on the seven-membered ring at δ 6.87 and 7.36 along with two methoxyl signals at δ 3.21 and 3.32. Similarly, the reaction of 2 with

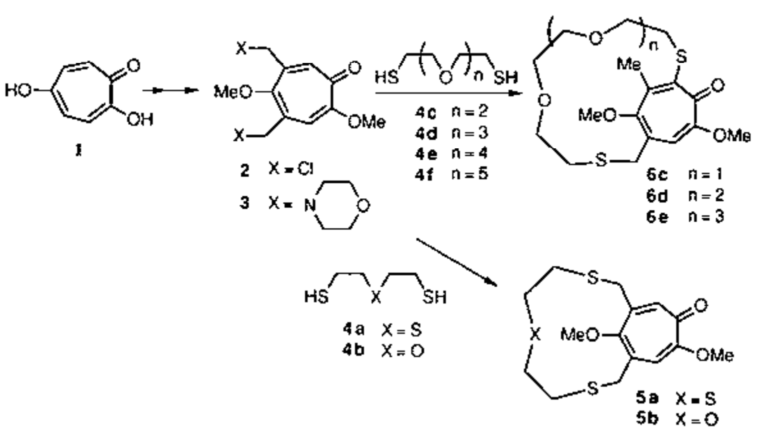

Scheme 2.

bis(mercaptoethyl) thioether (**4a**) gave **5a**, whose structure was deduced as depicted. The reaction of **2** with triethylene glycol bis(mercaptoethyl) ether (**4e**) gave another type of product **6e**, whose ^{1}H NMR spectrum showed three methyl singlet signals at δ 2.60, 3.40, and 3.89 along with one aromatic signal. Therefore, allylic substitution is evident. The position of the newly-generated methyl group was deduced from the chemical shift (δ 6.82) of the proton on the seven-membered ring which is appropriate for that of the vicinal position of the methoxyl group. Similar reactions of **2** with **4c,d** gave the corresponding derivatives **6c,d**.

There were two reaction modes depending on the chain length of **4**; the shorter ones gave S_N2 type products **5** via "path a", while the longer ones the S_N2' type products **6** via "path b". The chloromethyl group at C-4 in **2** was more reactive than that of C-6 because of the presence of the electron-donating methoxyl group at C-5.

Next, we focused our attention on preparing macrocyclic thioethers substituted on the C-3 and C-7 positions of troponoids. When an aqueous KOH solution of 5-butoxytropolone (**7**), prepared from **1**, reacts with formaldehyde, 5-butoxy-3,7-bis(hydroxymethyl)tropolone (**8**) is obtained [19]. After the methylation of **8** with diazomethane, 5-butoxy-3,7-bis(hydroxymethyl)-2-methoxytropone (**9**) was treated with thionyl chloride to give the corresponding 3,7-bis(chloromethyl) derivative **10**. The condensation of **10** with **4d** and **4e** gave the corresponding macrocyclic thioethers **11d** and **11e**, respectively. In these cases, the substitution reactions occurred at the side chains.

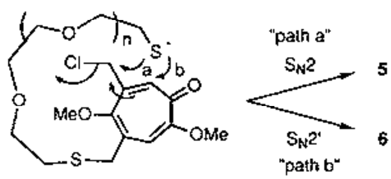

Scheme 3.

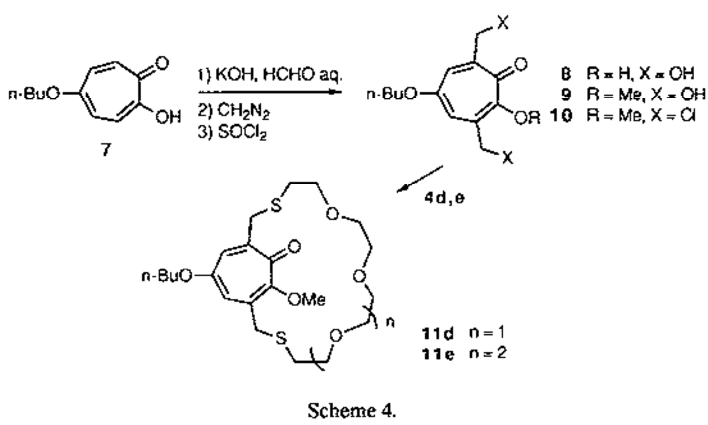

Scheme 4.

The ^1H NMR spectra are informative concerning the mobility of the macrocyclic ether rings. In the ^1H NMR spectrum of **6e**, the methylene protons on the carbon bearing the sulfur atom appeared as a broadened signal at δ 3.83, while the methylene protons of **6c** and **6d** appeared as magnetically non-equivalent *AB*-type signals at δ 3.12 and 4.37 for **6c** and δ 3.14 and 4.43 for **6d**, respectively. This clearly shows that the conformation of the macrocyclic rings in the shorter crown derivatives is fixed on the NMR time scale. The same is true for the case of **5**, prepared only from the short oligoethylene glycols; the methylene protons of both **5a** and **5b** appeared as *AB*-type signals.

The rotational barrier of the macrocyclic ether ring of **6d** could not be estimated since the variable temperature ^1H NMR spectra in DMF-d_7 up to 150 °C disclosed no indication of coalescence of the *AB*-type methylene proton signals. However, according to the ^1H NMR spectra of **6e** measured in CD_2Cl_2 at variable temperatures, the methylene proton signal on the adjacent carbon bearing the sulfur atom appeared at ca. δ 3.8 as a unified 2H signal at room temperature, but the signal began to split at −50 °C. At −90 °C, the doublet at the lower field of the *AB*-type quartet signals appeared at δ 4.40 ($J = 12.5$ Hz). Unfortunately, the counterpart at the higher field, estimated to be at ca. δ 3.2, was hidden underneath other signals (Fig. 1).

The chemical shift of the hidden methylene proton could be estimated to be at δ 3.24 from the chemical shift of the unified methylene protons at δ 3.82. The chemical shift difference of the methylene protons being about 313.2 Hz led to a rotational barrier of the macrocyclic ether ring of **6e** of 43.5 kJ mol^{-1} at −50 °C [18].

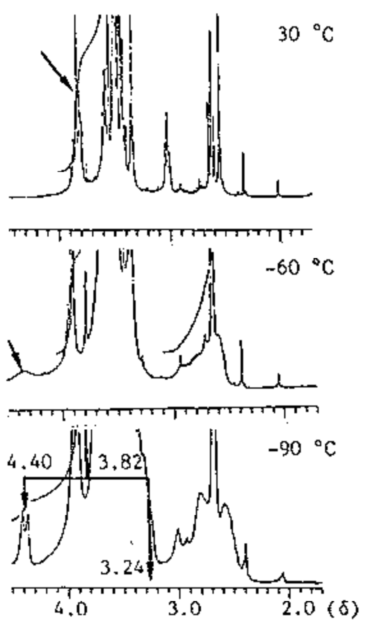

Fig. 1. Variable temperature NMR spectra of **6e** in CD_2Cl_2.

2.2. From hinokitiol

The Wittig-type rearrangement of 7-bromo-4-isopropyl-2-(4-nitrobenzyloxy) tropone (**12**) prepared from 7-bromohinokitiol with NaH at room temperature gave 7-bromo-2-(α-hydroxy-4-nitrobenzyl)-4-isopropyltropone (**13**) [20]. Upon treatment with *p*-tosyl chloride, **13** afforded 7-bromo-4-isopropyl-2-(α-tosyloxy-4-nitrobenzyl) tropone (**14**). The base condensation of **14** with **4a–f** gave macrocyclic dithiocrown ethers **15a–f**, respectively [21].

Catalytic reduction of **15e** with Pt-on-carbon catalyst afforded the 4-aminophenyl derivative **16e**. The pyridine-mediated condensation of **16e** with the acyl chloride of polyethylene carboxylic acid [22], derived from an oxidized polyethylene, in toluene gave the polymer supported dithiocrown compound **17e**. An anilide **18** was prepared from the polymer in order to compare the ability of the extract and the transport of metal ions with **17e** [23].

2.3. From tropones

Since the synthetic routes from 5-hydroxytropolone and hinokitiol required long steps, we planned to use readily-available 2,7-dibromotropone derivatives for the starting materials of troponoid dithiocrown ethers. The reaction of 2,7-dibromotropone (**19**) [24] and **4b–f** gave the 1:1 condensates **20b–f** and 2:2 condensates **21b–d** [25]. With longer bis(2-mercapto) ethers, 2:2 condensates were

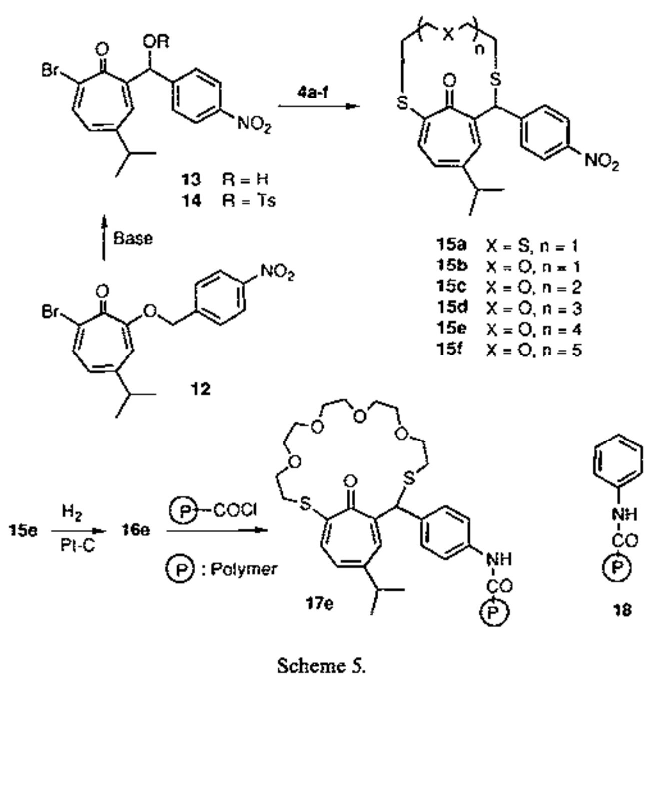

Scheme 5.

not formed due to the disadvantage in the entropy factor. The structures of new compounds were clarified by NMR spectroscopy. In ^{1}H NMR spectra, all **20b–f** had A_2B_2-type aromatic proton multiplets, and their overlapping ^{13}C NMR signals showed that **20b–f** were symmetric compounds. These spectroscopic features were also observed in the NMR spectra of **21b–d**.

In addition, the reaction of 7-bromo-4-isopropyl-2-(*p*-tolylsulfonyloxy)tropone (**22**) with **4b–f** gave the corresponding 1:1 condensates **23b–f** and 2:2 condensates **24b–d**. The ^{1}H NMR spectra of **23b–f** showed *ABX*-systems in the aromatic proton regions. Although the isopropyl group on the seven-membered ring made these derivatives unsymmetrical, the ^{13}C NMR spectral chemical shifts closely resembled each other. In this respect, the ^{1}H and ^{13}C NMR spectra of **24b–d** showed them to be regioisomeric 1:1 mixtures, which were chromatographically inseparable. The yields of the condensates are compiled in Scheme 6. Throughout the reactions, the yields of **20** and **21** were lower than those of **23** and **24**, but one-step formation of the dithiocrown derivatives should be satisfactory.

The NaH-mediated condensation of 2,4,7-tribromotropone (**25**) with **4b** and **4c** afforded the products **26–30**, respectively [26]. As shown in Scheme 7, the yields of the 2:2 condensates were low; **4b** gave a trace amount of 2:2 condensates **27** and **28**, while **4c** gave no 2:2 condensate. Both crystallines **27** and **28** were regioisomeric disubstituted products; the structural difference was confirmed by the ^{1}H NMR spectra. The methylene protons of the central ethylene groups at δ 3.79 (4H, t, $J=5.5$ Hz) and 3.84 (4H, t, $J=5.5$ Hz) of **27** show this to be the "*cis*"-isomer. On the other hand, the ^{1}H NMR spectrum of isomer **28** with a higher melting point showed

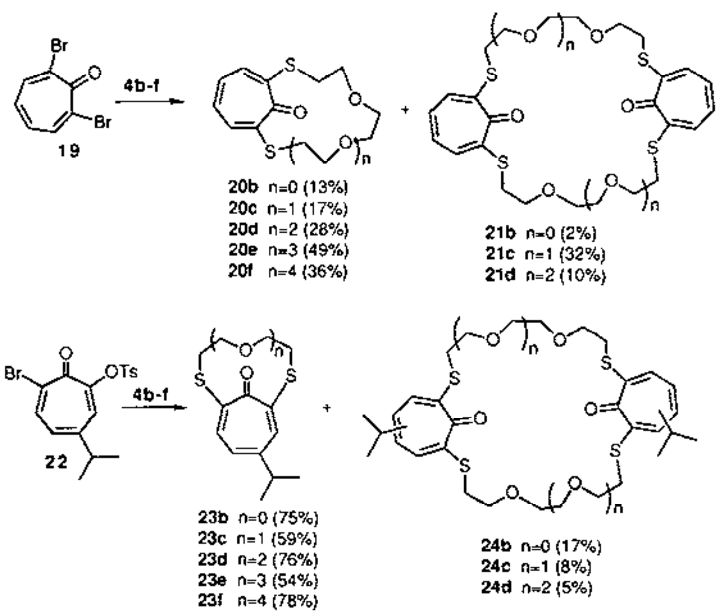

Scheme 6.

overlapping ethylene proton signals at δ 3.81 (4H, t, $J = 5.5$ Hz) and 3.83 (4H, t, $J = 5.5$ Hz) and thus is probably the "*trans*"-isomer. The by-product (**30**) was formed from the reaction of **4c** and **25**. An alternative structure (**30′**) was eliminated on the basis of the ^{1}H NMR chemical shifts of the aromatic protons.

The benzenoid dithiocrown ethers were prepared by the NaH-mediated condensation of 1,3-benzenedithiol (**31**) and pentaethylene glycol bis-*p*-toluenesulfonate (**32**). The ^{1}H NMR spectra of the 1:1 condensate **33** and the 2:2 condensate **34** and their overlapping ^{13}C NMR signals showed that they were symmetrical compounds.

3. Complex formation

3.1. 4,7-Disubstituted troponoid dithiocrown ethers 6

The cation-binding behavior of troponoid dithiocrown ethers was investigated by UV spectroscopy. Dithiocrown ethers **6** have absorption bands around 240, 295, 355, and 385 nm. When metal salts such as NaCl, KCl, and $AgNO_3$ were added to a MeOH solution of **6**, the spectra did not change. Upon addition of $HgCl_2$ the positions of the absorption bands changed slightly, and the extinction coefficient clearly increased, indicating complexation of **6e** and Hg^{2+}.

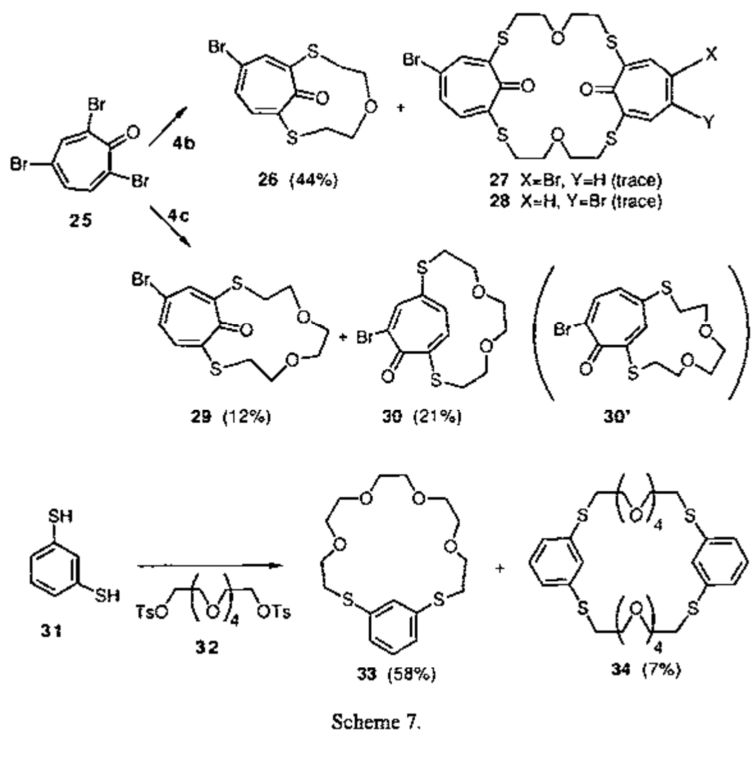

Scheme 7.

Next, we used NMR spectroscopy since it may offer a convenient tool to identify the metal-binding site of the complex. When an aqueous solution containing $HgCl_2$ was shaken with a $CDCl_3$ solution of **6**, Hg^{2+} was extracted into the $CDCl_3$ layer. The quantitative amount of Hg^{2+} was liberated simply by addition of 2 M HCl or aqueous NaCl (>20%), and the procedure can be repeated. The liberated Hg^{2+} was titrated by UV spectrometry as a 1,5-diphenylthiocarbazone (dithizone) complex. Particularly diagnostic for Hg^{2+}-complexed **6e** is the appearance of *AB*-type NMR signals at δ 3.66 and 3.90 ($J = 17.2$ Hz). All other NMR signals of the host molecules of the complexes experienced a downfield shift to some extent. The ratio of **6e** to Hg^{2+} was determined to be 1:1. Further, from an Hg^{2+}-containing 3% NaCl solution, Hg^{2+} was extracted by **6** as an inclusion complex. Moreover, from 3% $MgCl_2$ solution, Hg^{2+} was smoothly extracted by **6**. Thus, Na^+ and Mg^{2+}, abundant cations in sea water, did not interfere with Hg^{2+} extraction.

The NMR spectral change upon formation of a complex of Hg^{2+} with **6e** and **6d** disclosed information about the molecular structure (Figs. 2 and 3). At first, the methylene protons at δ 3.83 of **6e** became an *AB*-type pair of doublets at δ 3.66 and 3.90 ($J = 17.2$ Hz) in contact with Hg^{2+}. This is due to a freezing of the conformation, which should be a result of complex formation with Hg^{2+}. In the case of **6d**, the methylene signals showed down-field shifts upon the complex formation, δ 3.12 and 4.37 to 3.22 and 4.40, respectively. It is clear that the quasi-axial proton, appearing at a higher field, suffered substantial influence from the complex formation.

However, complex formation did not cause significant changes in the physical and chemical properties of the troponoid structure; a change from δ 179.1 to 178.2 in the chemical shift of the ^{13}C NMR spectrum of C=O of **6e** is very small.

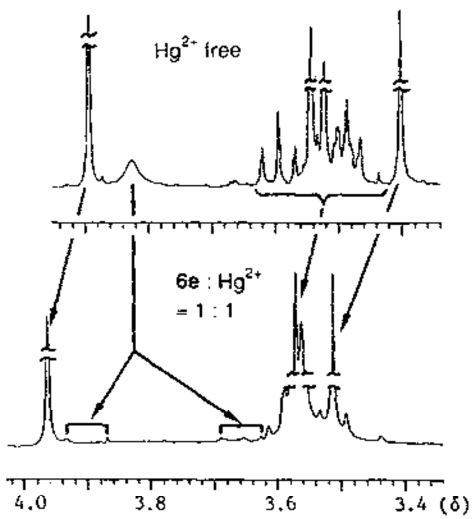

Fig. 2. Change in ^1H NMR spectrum of **6e** caused by addition of Hg^{2+} (adapted from Ref. 17).

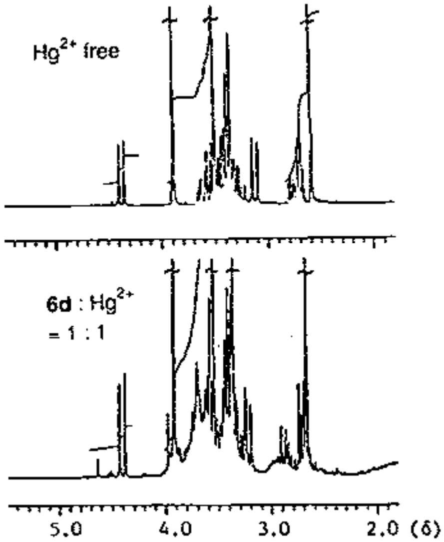

Fig. 3. Change in ^{1}H NMR spectrum of **6d** caused by addition of Hg^{2+}.

3.2. 3,7-Disubstituted troponoid dithiocrown ethers 11d and 11e

Complex formation of **11d** with $HgCl_2$ showed all the NMR signals shifted to a lower field. The broad signals between δ 3.1 and 3.4 and between δ 4.3 and 4.6 of **11d** became triplets upon complexation. These spectral features indicated a freezing of the conformation. The IR spectrum of the complex of **11d** with Hg^{2+} showed that the absorption bands of C=O and C=C were shifted to the lower frequencies by 10–17 cm^{-1}. In the complex of **11d** with $HgCl_2$ the carbonyl oxygen may interact with Hg^{2+} to form complexes [19].

On the contrary, the NMR spectrum of **11e** showed rather more sharp signals than that of **11d**, which indicated that the conformation of **11e** with the longer chain is more mobile within the NMR time scale [19]. The NMR spectrum of the Hg^{2+} complex of **11e** also showed that all of the signals shifted to the lower field.

3.3. 2,7-Disubstituted troponoid dithiocrown ethers 20 and 23

The tropone rings of the dithiocrown ethers **20** and **23** are more electron-rich than **6** and **11** since two sulfur atoms are directly connected to the tropone ring. Even **20b** and **23b**, whose cavity sizes are not large enough to include Hg^{2+}, formed complexes with Hg^{2+}. Fig. 4 shows Hg^{2+}-induced changes in the chemical shift of H-3 of the tropone ring, among which **20e** showed the largest change [25]. Interestingly, while the ethylene proton signals in the Hg^{2+}-complex of **20e** shifted to lower field, the signal of H-3 shifted to higher field. The low field shift of the ethylene proton signals was easily explained by the complexation with Hg^{2+}. The high field shift of the aromatic protons must be explained by a decrease of the

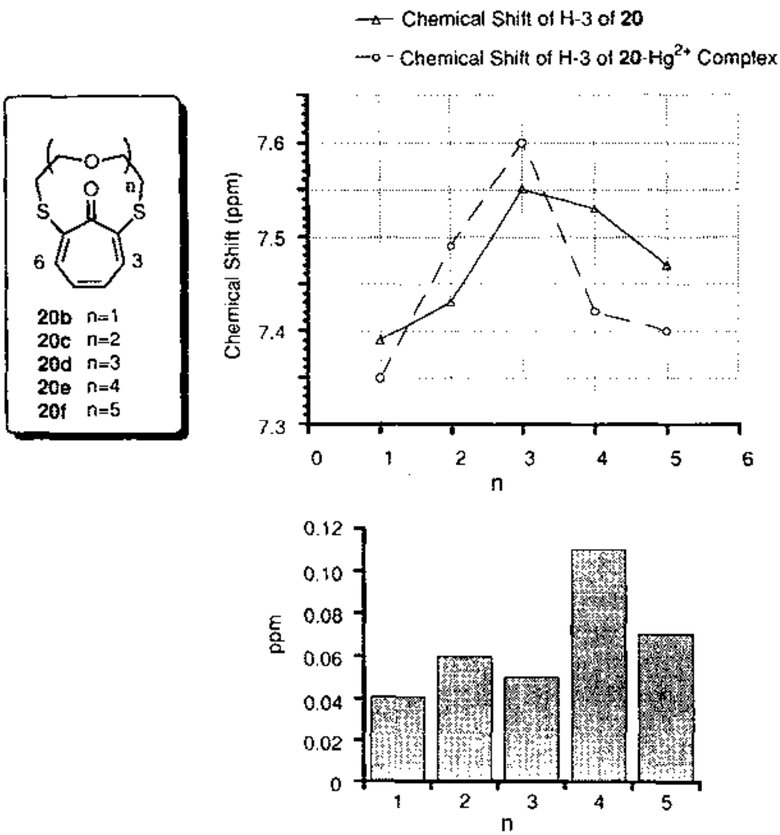

Fig. 4. Hg^{2+}-induced changes in the ^{1}H NMR chemical shifts of **20**.

electron-density of the tropone ring due to the complexation. The cavity size of **20e** was estimated to be 2.9–3.5 Å from the CPK model. The sizes of **20f** and **20d** were 4.8–5.2 and 1.7–2.3 Å, respectively. The size of **20e** is, therefore, most appropriate for the size (2.20 Å) of Hg^{2+}. The attempted complex formation of **20e** with various metal ions, i.e., among them the alkaline metals, alkaline earth metals, and some transition metal ions, Li^{+}, Na^{+}, Mg^{2+}, Ca^{2+}, Ba^{2+}, Co^{2+}, Ni^{2+}, Fe^{3+}, Co^{2+}, Zn^{2+}, Cd^{2+}, and Ag^{+}, showed no spectral changes in the ^{1}H NMR.

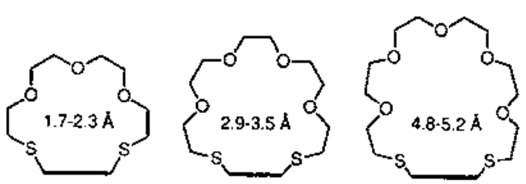

20d **20e** **20f**

Scheme 8.

Next, a standard aqueous solution containing $HgCl_2$ was shaken with a $CHCl_3$ solution of **20b–f** and the aqueous layer was titrated photometrically at 490 and 610 nm in phosphate buffer with added dithizone solution. Fig. 5 shows the molar ratios of the extracted Hg^{2+}; **20e** showed the highest value, 0.98, while the others showed lower values, 0.29 for **20b**, 0.35 for **20c**, 0.24 for **20d**, and 0.71 for **20f**.

Thus, a size dependency for complex formation was again confirmed. Among the homologues, **20e** was most effective with respects to extraction, and significant differences were noticed between **20e** and others, such as **20f**. This is attributable to an appropriate size of the cavity in **20e**. In parallel, **23e** was most effective among the homologues. At the same time, the rates of the liberation of Hg^{2+} are very much improved, reflecting a marked decrease of basicity of the sulfur atoms, which are directly connected to the aromatic ring; the previous examples required almost twice as long as the complexation period for complete liberation of Hg^{2+} [14,18].

*3.4. 2,7-Disubstituted troponoid dithiocrown ethers **20**, **21c,d**, and **26** and 4,7-disubstituted troponoid dithiocrown ether **30** with thiocyanates*

UV-vis spectra of troponoid dithiocrown ethers **20**, **21c**, **d**, **26**, and **30** were changed by addition of various thiocyanates (100 equiv.) as shown in Table 1 [26]. Dithiocrown ethers **20b–d**, **26**, and **30** with a smaller cavity did not show significant spectral changes upon the addition of various salts, while dithiocrown ethers **20e** and **20f** with a larger cavity showed appreciable spectral changes upon the addition of Ca^{2+}, Ba^{2+}, Hg^{2+}, and Cd^{2+}. The changes were small when Li^+, Na^+, K^+, NH_4^+, Mg^{2+}, and Zn^{2+} were added. Fig. 6 shows the spectral changes of **20e** in CH_3CN upon the addition of various metal salts. The absorption band at 399 nm of **20e** decreased with increasing concentration of the complexes. As can be seen from Fig. 7, the decrease in intensity of the band is accompanied by an increase in the absorption in the longer wavelength region. The spectral changes of **20e** upon addition of Ca^{2+} were similar to those observed by the addition of Ba^{2+}, Mg^{2+}, Zn^{2+}, Cd^{2+}, and Hg^{2+}. However, upon addition of Li^+, Na^+, K^+, and NH_4^+,

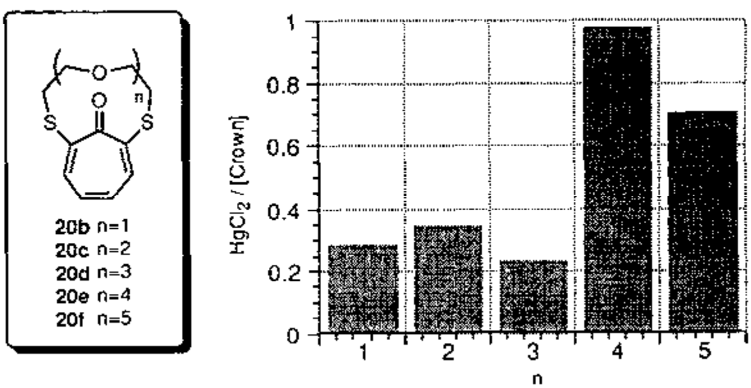

Fig. 5. Relative ratio of extracted Hg^{2+} by **20**.

Table 1
Salt-induced absorption spectral changes of thiacrown ethers in CH_3CN

	20b	**20c**	**20d**	**20e**	**20f**	**21c**	**21d**	**26**	**30**
LiSCN	−	−	−	−	−	−	−	−	−
NaSCN	−	−	−	−	−	−	−	−	−
KSCN	−	−	−	−	−	−	−	−	−
NH_4SCN	−	−	−	−	−	−	−	−	−
$Ca(SCN)_2$	−	−	−	++	++	+	++	−	−
$Mg(SCN)_2$	−	−	−	+	+	−	−	−	−
$Ba(SCN)_2$	−	−	−	++	++	+	++	−	−
$Zn(SCN)_2$	−	−	−	+	+	+	−	−	−
CdI_2	−	−	−	+	++	++	++	−	−
$Hg(SCN)_2$	−	−	−	++	++	+	−	−	−

++ and +, changed strongly and weakly, respectively; −, no appreciable change. Spectral conditions: crown ether (0.02 mM l^{-1}), metal salts (2.0 mM l^{-1}) in CH_3CN at 298 K.

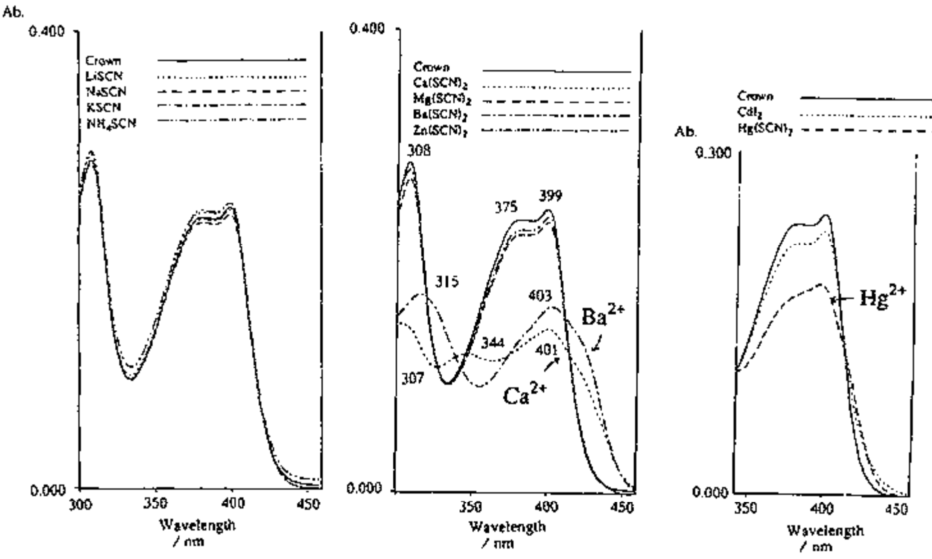

Fig. 6. UV spectral changes of **20e** by addition of various metal salts.

there was no additional longer wavelength absorption. The spectral changes were dependent upon the metal ions added, which suggested that the binding sites were dependent on the metal ions.

4. Transport

The transport experiments were performed using a U-type cell, shown in Fig. 8. When an aqueous solution of $HgCl_2$ (aq. I) was brought into contact with a $CHCl_3$

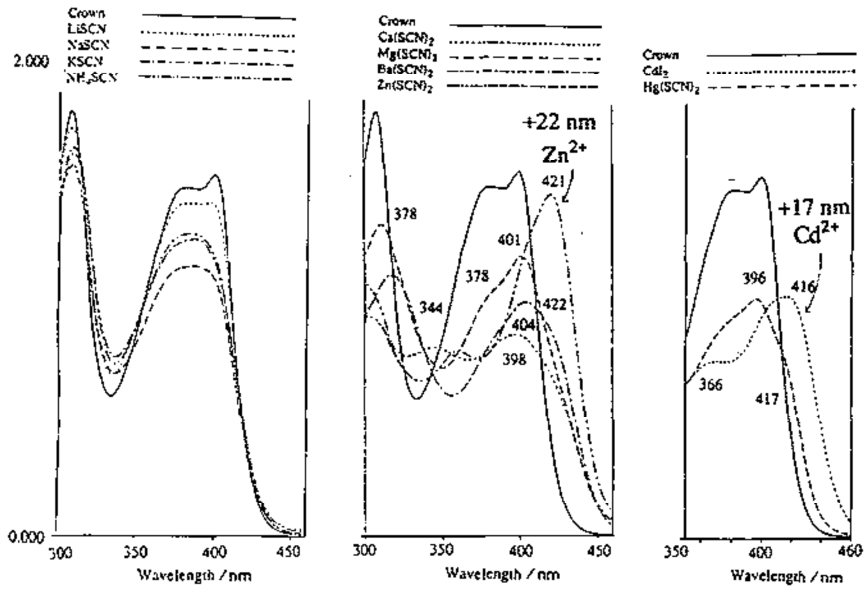

Fig. 7. UV spectral changes of **20e** by addition of excess metal salts.

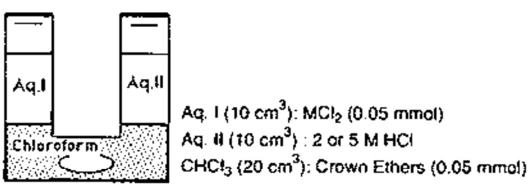

Fig. 8. U-type cell used for transport experiments.

solution of **6e**, stirring with a magnetic bar at 20 °C, the concentration of Hg^{2+} in the aq. I decreased. The Hg^{2+} was transported to the $CHCl_3$ layer and could be extracted by aqueous 2 M HCl (aq. II). After 70 h, the Hg^{2+} was extracted quantitatively into the aq. II as shown in Fig. 9. This process could be carried out repeatedly with perfect reproducibility.

From ^1H and ^{13}C NMR spectra, metal salts such as LiBr, NaBr, AgBr, $MgCl_2$, $CoCl_2$, $NiCl_2$, $CuCl_2$, $ZnCl_2$, $SrCl_2$, $CdCl_2$, $BaCl_2$, or $FeCl_3$ were not extracted into the $CHCl_3$ solution from the aqueous solution. The attempted transport of K^+ using the same equipment at 25 °C for 100 h under the same conditions as above with Hg^{2+} did not take place.

In addition, Cu^{2+} did not interfere with the extraction or transport of Hg^{2+} on the basis of ^1H NMR evidence. This was clearly shown when the transport experiment with Hg^{2+} was carried out in the presence of Cu^{2+}; an aqueous solution of $HgCl_2$ and $CuCl_2$ was treated with a $CHCl_3$ solution of **6e** and 2 M HCl; all the Hg^{2+} was dissolved in the organic layer after 40 h. After 60 h, 75% of Hg^{2+} was extracted into

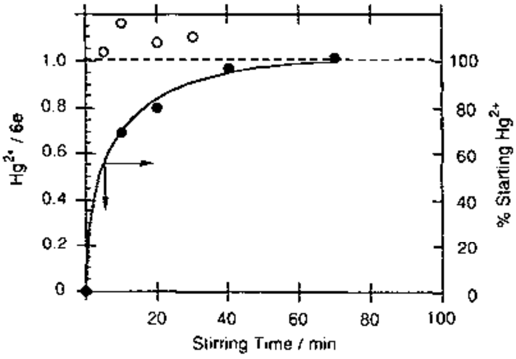

Fig. 9. Dependence on stirring time of ratio of Hg^{2+} and **6e** in the complex (○) and concentration of Hg^{2+} by reverse-extraction with 2 M HCl (●) (adapted from Ref. 17).

the dilute HCl solution. However, Cu^{2+} remained quantitatively in the initial solution. This high selectivity for Hg^{2+} in the transport experiment is interesting (Fig. 10).

Similarly, **15e** extracted and transferred Hg^{2+} from a mixture containing Cu^{2+} in distilled water (Figs. 11 and 12).

In the transport experiment of Hg^{2+} for the 2:2 condensate **21c**, the Hg^{2+} was not extracted quantitatively by aqueous 2 M HCl even after a week. In the $CHCl_3$ solution, 5% of Hg^{2+} remained and could be extracted by aqueous 5 M HCl. Fig. 13 shows the result of the Hg^{2+} transport with **21c** using 2 M HCl and 5 M HCl. The stronger acidity enhanced the transport of Hg^{2+}. This result indicates that protonation of the carbonyl group of **21c** is important to release Hg^{2+}.

Fig. 14 shows the transport experiments of Hg^{2+} for **20e** using 2 M and 5 M HCl, where the stronger acidic medium facilitates the liberation of Hg^{2+} to enhance the whole transport and extraction processes. Fig. 15 shows the transport experiments of Hg^{2+} for **20b–f**. The dithiocrown ether **20e** was most effective in Hg^{2+} transport and the transport rates of other **20** species are similar. Dithiocrown ether **20f** with

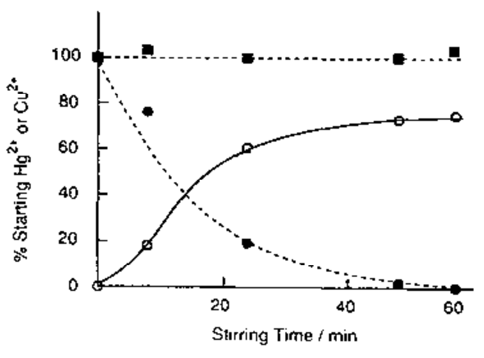

Fig. 10. Carrier-mediated Hg^{2+} transport with **6e** in the presence of Cu^{2+}; ○, Hg^{2+} transported; ●, Hg^{2+} remaining; ■, Cu^{2+} remaining (adapted from Ref. 17).

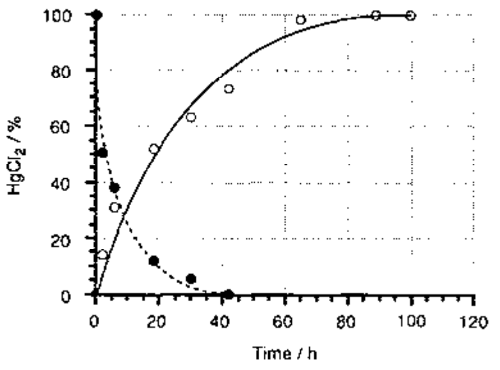

Fig. 11. Extraction and transfer experiments of Hg^{2+} with **15e**; ●, Hg^{2+} remaining; ○, Hg^{2+} transported.

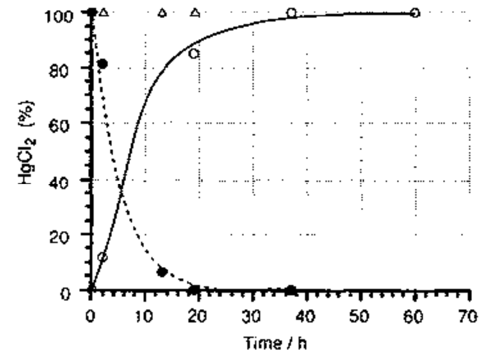

Fig. 12. Extraction and transfer experiments of Hg^{2+} with **15e** in the presence of Cu^{2+}; ○, Hg^{2+} transported; ●, Hg^{2+} remaining; △, Cu^{2+} remaining.

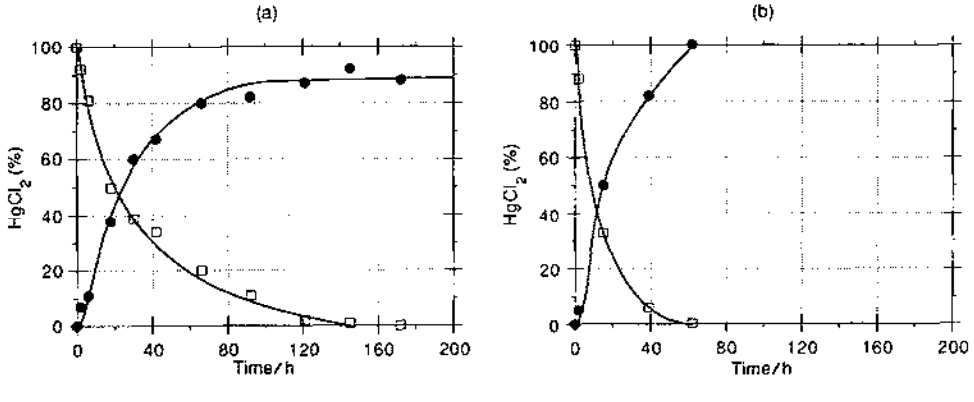

Fig. 13. Transport of Hg^{2+} with **21c** using 2 M HCl (a) and 5 M HCl (b); □, Hg^{2+} remaining; ●, Hg^{2+} transported.

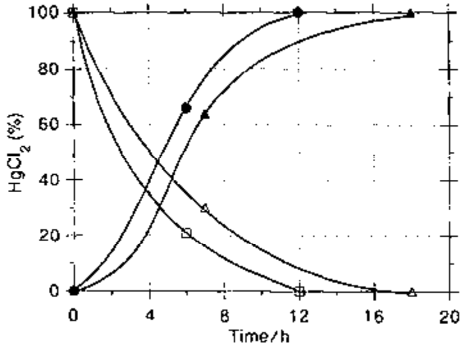

Fig. 14. Transport of Hg^{2+} with **20e** using 2 M HCl and 5 M HCl; △, Hg^{2+} remaining in 2 M HCl; ●, Hg^{2+} transported in 2 M HCl; □, Hg^{2+} remaining in 5 M HCl; ▲, Hg^{2+} transported in 5 M HCl.

the largest cavity was less effective in transport than **20e**. The relationship between the rates of transport and the chain length of **20b–f** is shown in Fig. 16. The size of the cavity of **20e** fits well the size of Hg^{2+}. This is consistent with the result obtained in complex formation.

Next, the transport selectivity for Hg^{2+} over Cu^{2+} was investigated with **20e**; Fig. 17 shows representative results of the transport of Hg^{2+}; e.g., by means of **20e**, Hg^{2+} is transferred selectively and smoothly, while the coexisting Cu^{2+} remained in the original solution [17,21].

The ^1H NMR spectral changes shown in Table 2 [26] reveal the complex formation of **33** with $HgCl_2$, $AgNO_3$, and $CdCl_2$. The selectivity of **33** was poorer than that of **20e**, which showed the highest selectivity for Hg^{2+} as already shown. The transport rates for **20b–f**, **26**, **30**, and **33** are listed in Table 3. The rates of **26** and **30** were nearly the same as those of **20b** and **20c**. In the Hg^{2+} transport experiment, the rate of **33** was less than 40% that for **20e**. The results are summarized in Fig. 18. It is also noteworthy that the rate of release of Hg^{2+} with **33** from the membrane to the receiving phase is slower than those of **20e** and **20f**. Thus, the tropone function plays an important role in the release of Hg^{2+} to the receiving phase. The result clearly shows that protonation is responsible for generating the 6π-cationic system and assisting the release of Hg^{2+} by Coulomb repulsion in the Hg^{2+} complex.

The proposed transport mechanism is shown in Fig. 19. The Hg^{2+} forms a complex, which is soluble in the solvent of the liquid membrane, $CHCl_3$. The complexes dissociated immediately when exposed to a strong acid because of the rapid generation of a tropylium cation. From measurement of the pH of the aq. I phase of the U-type cell, the proton transport can be followed [27]. The tropone system assisted the release of the metal ion from the complex.

In order to apply the unique Hg^{2+} affinity of these troponoid dithiocrown ethers, we have prepared the polymer-supported dithiocrown ether **17e**. After the polymer **17e** was soaked in a standard $HgCl_2$ solution, **17e** was filtered off, washed with water, and dried. The dried **17e** was washed with 2 M HCl. Quantitative analysis of

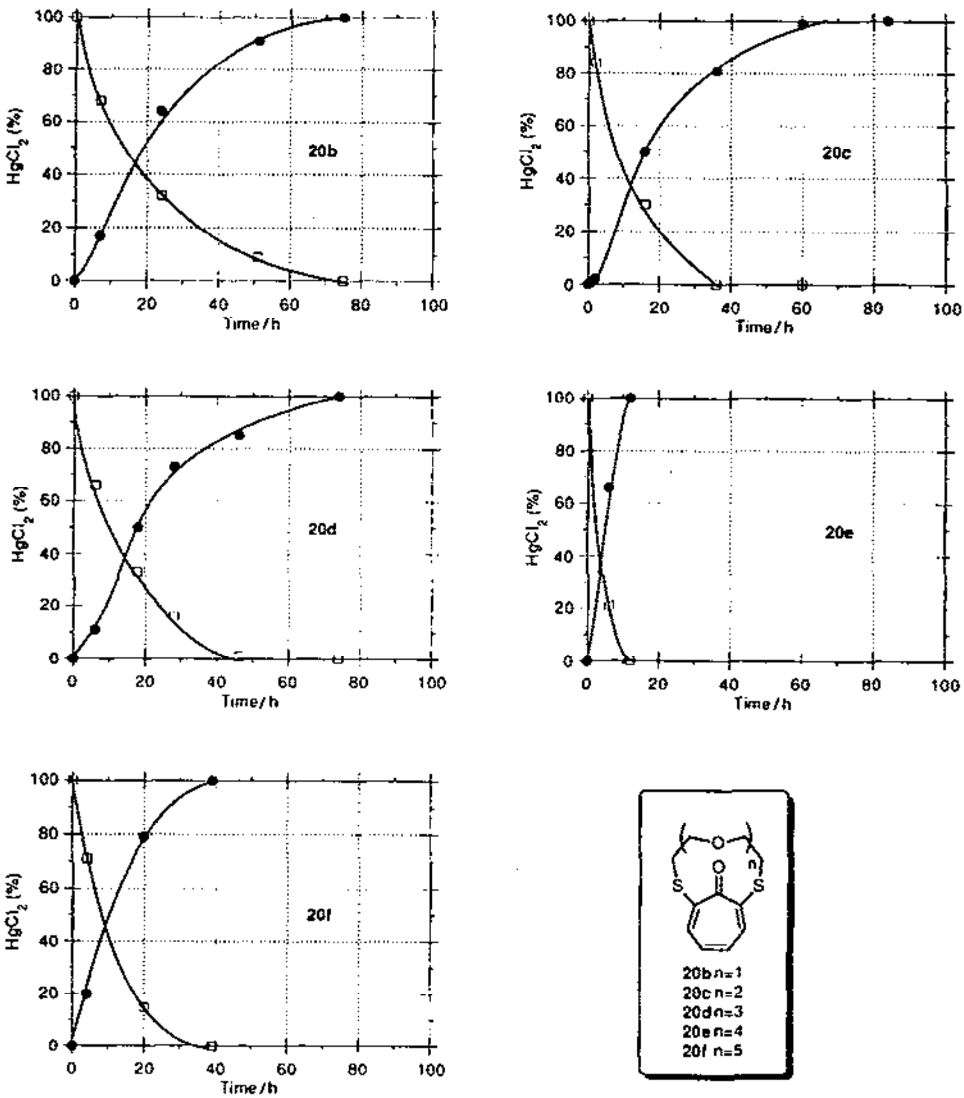

Fig. 15. Extraction and transfer experiments of Hg^{2+} with 20; ●, Hg^{2+} remaining; □, Hg^{2+} transported.

the Hg^{2+} transferred into the HCl solution revealed that **17e** retained ca. 25% activity after fixation on the polymer. An anilide **18** failed to extract Hg^{2+}. Therefore, the extraction of Hg^{2+} with the polymer **17e** is due to the presence of the dithiocrown ether part, and is not due to physical adsorption. The successful preparation of polymer-supported crown ethers which can capture Hg^{2+} is of great interest from the environmental point of view.

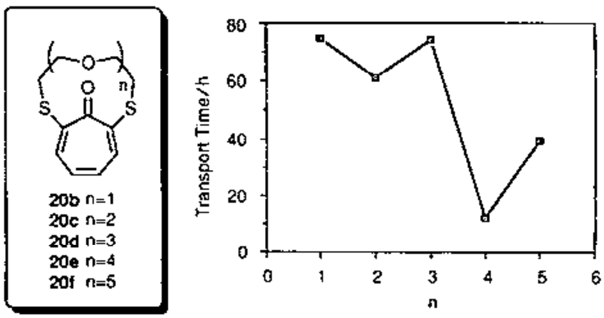

Fig. 16. Transport time of Hg^{2+} by **20**.

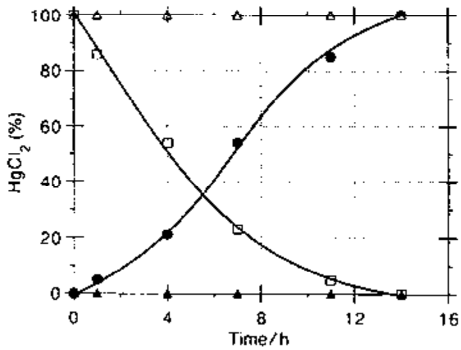

Fig. 17. Selective transport of Hg^{2+} with **20e**; ☐, Hg^{2+} remaining; ●, Hg^{2+} transported; △, Cu^{2+} remaining; ▲, Cu^{2+} transported.

Table 2
NMR spectral changes of **33** upon addition of various metal ions

Free	$HgCl_2$	$AgNO_3$	$CdCl_2$
^{1}H NMR ($CDCl_3$)	^{1}H NMR ($CDCl_3$)	^{1}H NMR ($CDCl_3$)	^{1}H NMR ($CDCl_3$)
δ 7.49 (1H, brs)	δ 7.60 (1H, brs)	δ 7.53 (1H, brs)	δ 7.51 (1H, brs)
7.11–7.20 (3H, m)	7.12–7.22 (3H, m)	7.12–7.22 (3H, m)	7.11–7.20 (3H, m)
3.69 (4H, t, J=6.8 Hz)	3.68 (4H, t, J=6.6 Hz)	3.68 (4H, t, J=6.6 Hz)	3.69 (4H, t, J=6.8 Hz)
3.59–3.64 (12H, m)	3.64–3.65 (12H, m)	3.64 (12H, s)	3.59–3.65 (12H, m)
3.14 (4H, t, J=6.8 Hz)	3.27 (4H, t, J=6.6 Hz)	3.15 (4H, t, J=6.6 Hz)	3.15 (4H, t, J=6.8 Hz)

5. Association constant

5.1. UV spectrometry

Association constants were determined using the Benesi–Hildebrand approximate equation [28] and the non-linear curve fitting method [29,30] from the absorbance change in the UV spectra (CH_3CN) or the chemical shift change in the ^{1}H NMR

Table 3
Transport rate for Hg^{2+} for various crown ethers

Crown ethers	Transport rate ($\mu M\ h^{-1}$)
20b	1.2
20c	1.7
20d	0.9
20e	5.5
20f	2.3
26	1.2
30	1.2
33	2.0

Transport rate: (transport quantity/time) after 6 h at 298 K.

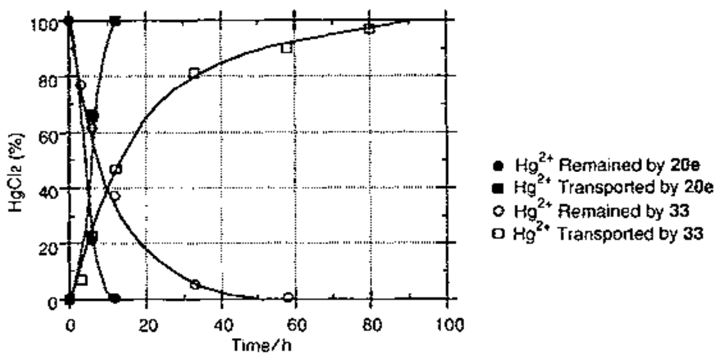

Fig. 18. Comparison of transport experiments of Hg^{2+} with **20e** and **33**.

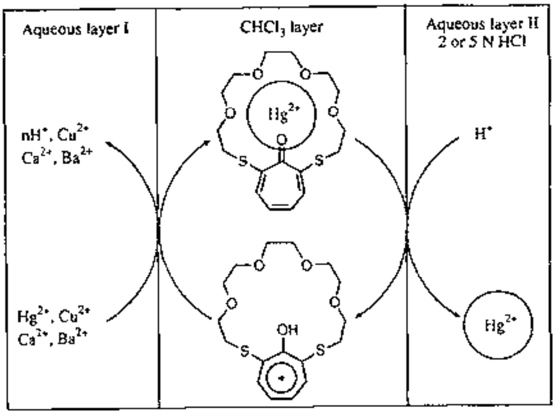

Fig. 19. Transport mechanism.

(CD_3CN) with the titration of metal salts at 298 K [26]. Fig. 20 shows the Benesi–Hildebrand plots of **20e** by the addition of Li^+ in CH_3CN. The stoichiometry of the complex should be 1 : 1. The association constant K_s was calculated from the slope. Similarly, the association constants for other ions, Na^+, K^+, and $NH_4{}^+$, were determined by the Benesi–Hildebrand method. Association constants of **20e** for complexes formed by the addition of Ca^{2+}, Ba^{2+}, Zn^{2+}, Mg^{2+}, Cd^{2+}, and Hg^{2+} were calculated from the titration curves. The dithiocrown ether **20e** showed the following selectivity: $Na^+ < K^+ < NH_4{}^+ < Li^+ < Mg^{2+} < Zn^{2+} < Cd^{2+} < Hg^{2+} < Ba^{2+} < Ca^{2+}$ in CH_3CN. Fig. 21 shows the curve-fitting plot of change in absorbance upon the addition of salts. These results are summarized in Table 4. The observed larger complexation constants for Ca^{2+} and Ba^{2+} being greater than Hg^{2+} are not apparently consistent with the results from the transport experiment, which showed that only Hg^{2+} was transported. Probably, the complexes of Ca^{2+} and Ba^{2+} are not soluble in $CHCl_3$, the solvent for the transport experiments. Failure to

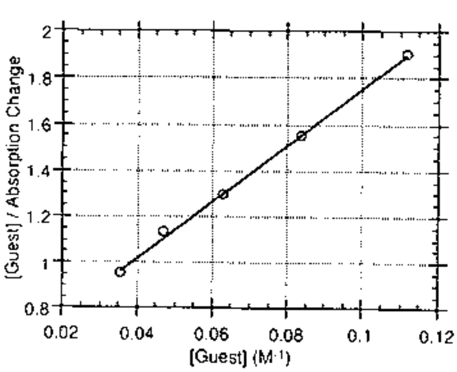

Fig. 20. Benesi–Hildebrand plot for the mixture of **20e** and LiSCN.

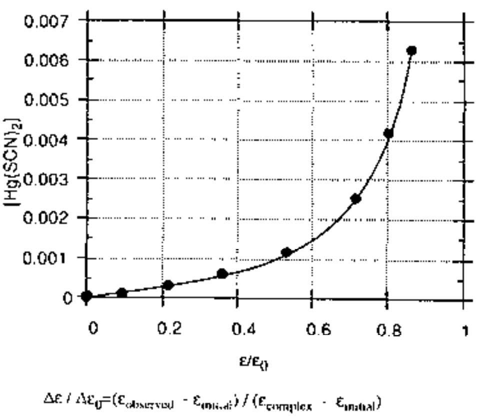

Fig. 21. Titration curve showing the change in intensity in the UV spectra upon mixing **20e** and $Hg(SCN)_2$.

Table 4
K_s values determined by ^{1}H NMR and UV spectrum titration in CH_3CN or CD_3CN

	Method	Salts	K_s	Log K_s	R^a
20e	a	LiSCN	23	1.36	0.999
	a	NaSCN	4	0.60	0.992
	a	KSCN	18	1.26	0.999
	a	NH_4SCN	21	1.32	0.994
	b	$Ca(SCN)_2$	7250	3.86	0.999
	b	$Mg(SCN)_2$	20	1.30	0.999
	b	$Ba(SCN)_2$	5541	3.73	0.999
	b	$Zn(SCN)_2$	24	1.37	0.999
	b	CdI_2	73	1.86	0.999
	b	$Hg(SCN)_2$	1020	3.01	0.999
	c	$Hg(SCN)_2$	1090	3.04	0.999
20f	c	$Hg(SCN)_2$	354	2.55	0.999
33	c	$Hg(SCN)_2$	516	2.71	0.995

a, Benesi–Hildebrand equation (UV spectrum); b, curve-fitting method (UV spectrum); c, ^{1}H-NMR titration. ^{a}R factor for curve fitting. Conditions: CH_3CN or CD_3CN at 298 K.

rationalize the results in terms of the log K_s (CH_3CN) values suggests that the log K_s ($CHCl_3$) values for the interaction between Hg^{2+} and **20e** in these cases may be larger than those of Ca^{2+} or Ba^{2+}.

The absorption maximum of **20e** was shifted largely by complexation as shown in Table 5. The largest shift was observed when Zn^{2+} was complexed with **20e**. The metal ion selectivities observed from the λ_{max} shifts do not correlate with the association constants of the complexes in each case. This fact is predictable from the results reported by Vögtle [31].

5.2. ^{1}H NMR spectrometry

New signals separated from those of the uncomplexed **33** when $Hg(SCN)_2$ was added. A triplet signal for the ethylene protons adjacent to the sulfur atom of **33**

Table 5
Absorption maximum shifts of various **20e** complexes in acetonitrile

Metal ions	λ (nm) (ε)	$\Delta\lambda$ (nm)
20e	399 (11400)	–
Mg^{2+}	401 (8800)	2
Ca^{2+}	398 (6400)	1
Ba^{2+}	404 (7400)	5
Zn^{2+}	421 (10800)	22
Cd^{2+}	416 (7700)	17
Hg^{2+}	396 (7600)	3

$\Delta\lambda = |\lambda_{complex} - 399|$ at 298 K in CH_3CN.

appeared at δ 3.12, which shifted to the lower field at δ 3.32 due to the formation of the **33**–Hg^{2+} complex (Fig. 22). The association constant of **33** determined using the integral ratio in the ^{1}H NMR spectrum (Fig. 23) was 515 M^{-1}, which is smaller than that of **20e** (1090 M^{-1}), determined by the change in chemical shift in the ^{1}H NMR spectrum (Fig. 24). It is consistent with the result (1023 M^{-1}) determined by the UV spectra (Fig. 21). The association constant of **20f** with Hg^{2+} with the larger

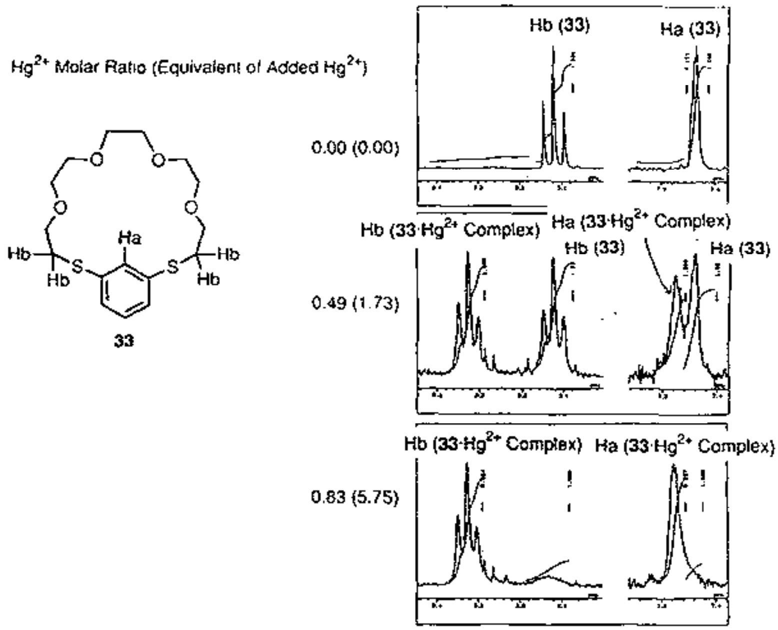

$$\mathrm{Hg^{2+}\ Molar\ Ratio} = \frac{[\mathbf{33}\cdot\mathrm{Hg^{2+}\ Complex}]}{[\mathbf{33}+\mathbf{33}\cdot\mathrm{Hg^{2+}\ Complex}]}$$

Fig. 22. ^{1}H NMR spectral changes of **33** by addition of $Hg(SCN)_2$.

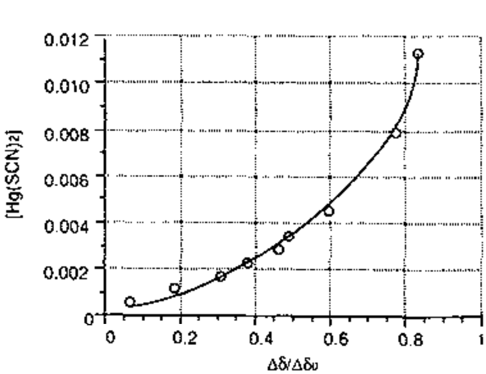

Fig. 23. ^{1}H NMR titration curve of **33** for $Hg(SCN)_2$.

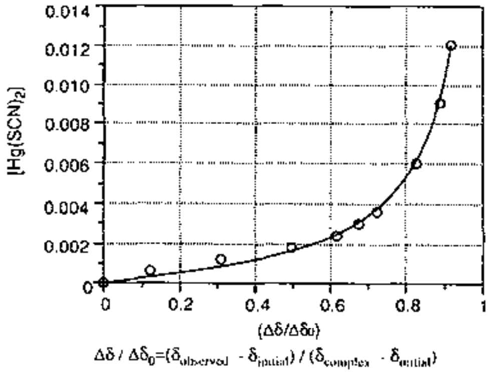

Fig. 24. ^{1}H NMR titration curve for the mixture of **20e** and $Hg(SCN)_2$.

cavity size than **20e** was lower than that of **20e**. This result is consistent with the transport data observations [17].

6. Stereostructure of the mercurophilic dithiocrown derivative

Fortunately, **20b** and its mercury complex crystallized nicely. According to the X-ray diffraction structural analysis [25], the mercury complex of **20b**, a monoclinic crystal with cell dimensions of $a = 11.693(1)$, $b = 15.083(3)$, $c = 10.349(1)$ Å, and $\beta = 98.000(8)°$ with $P2_1/a$, showed that its structure contains two mercury atoms per one **20b** as has been confirmed at the final stage, where the R factor is 0.047. It is noteworthy that two Hg^{2+} are coordinated respectively with one carbonyl oxygen and one sulfur atom as depicted in Fig. 25; **20b**, whose cell dimensions were $a = 13.400(2)$, $b = 28.763(4)$, and $c = 12.036(2)$ Å with *Pbca*, had a non-planar seven-membered ring and the carbonyl group deviated particularly from the plane set by adjacent C=C bonds, by as much as 32.0°, while the deviation in the mercury complex of **20b** was 25.9°, as shown in Fig. 26.

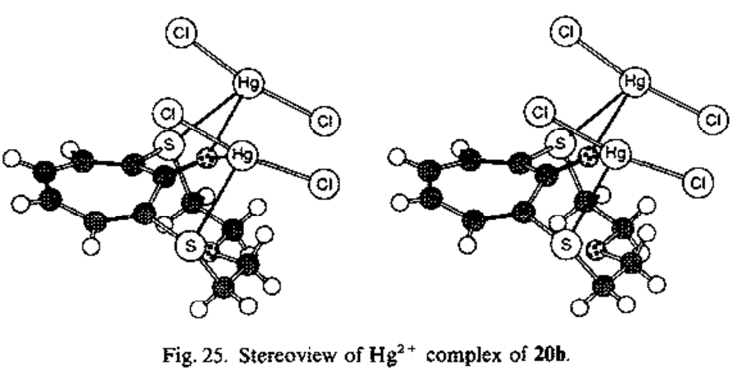

Fig. 25. Stereoview of Hg^{2+} complex of **20b**.

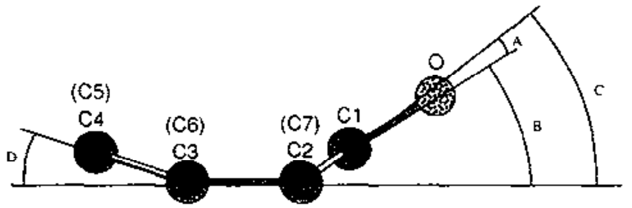

20b	Hg^{2+} Complex	
Angle A: 1.6	Angle A: 3.6	A = C1-O // C1-C2-C7
Angle B: 32.0	Angle B: 25.9	B = C1-O // C2-C3-C6-C7
Angle C: 33.5	Angle C: 29.5	C = C1-C2-C7 // C2-C3-C6-C7
Angle D: 14.4	Angle D: 12.2	D = C2-C3-C6-C7 // C3-C4-C5-C6

Fig. 26. Schematic side-view of tropone nucleus of **20b** and Hg^{2+} complex.

Further X-ray structural analyses of **20** and their mercury complexes will be important subjects to unravel the complexation of troponoid dithiocrown ethers.

7. Conclusions

Troponoid dithiocrown ethers displayed a unique selectivity towards Hg^{2+}, one of the most harmful heavy metal ions. Among troponoid dithiocrown ethers, **20e** was the most effective mercurophilic dithiocrown ether and a more effective Hg^{2+} transport carrier than the benzenoid dithiocrown ether **33** with a similar cavity size. While 19-dithiocrown-6-ether [9] and 16-dithiocrown-5-ether [9] formed complexes with Hg^{2+}, acid treatment with 2 M HCl did not liberate Hg^{2+}. Therefore, it can be concluded that the tropone ring assisted the release of the metal ion from the complex by Coulomb repulsion, since the protonation generates the 6π-cationic system. Furthermore, the changes in the UV spectra of the troponoid thiocrown ethers upon the addition of ions can be used as a probe to analyze complex formation. These are characteristic of troponoids.

It has become apparent that the cavity size of the dithiocrown ethers is an important parameter for effective extraction and transport of Hg^{2+}, but the derivatives with a smaller ring still extract and transport Hg^{2+}. It is now suggested that Hg^{2+} does not penetrate deeply into the dithiocrown rings, and this geometry plays a positive role in facilitating the reversible complexation.

References

[1] C.J. Pedersen, J. Am. Chem. Soc., 89 (1967) 2495; C.J. Pedersen, J. Am. Chem. Soc., 89 (1967) 7017.

[2] Recent rewiews: for examples, T. Wang, J.S. Bradshaw and R.M. Izatt, J. Heterocyclic. Chem., 31 (1994) 1097; H.C. Visser, D.N. Reinhoudt and F. de Jong, Chem. Soc. Rev., (1994) 75.

[3] T. Nozoe, Sci. Rep. Tohoku Univ. I, 34 (1950) 199; W. von E. Doering and L.H. Knox, J. Am. Chem. Soc., 73 (1950) 828; J.M. Robertson, J. Chem. Soc., (1951) 1222; Y. Oka and S. Matsuo, Bunseki Kagaku, 7 (1958) 215.

[4] T. Nozoe, K. Takase and H. Matsumura in M. Kotake (ed.), Comprehensive Organic Chemistry, Vol. 13, Asakura Shoten, Tokyo, 1959.
[5] F. Pietra, Chem. Rev., 73 (1973) 293.
[6] T. Nozoe, Yakugaku, 3 (1949) 174.
[7] T. Asao and Y. Kikuchi, Chem. Lett., (1972) 423.
[8] C.J. Pedersen, J. Org. Chem., 36 (1971) 254.
[9] J.S. Bradshaw, R.A. Reeder, M.D. Thompson, E.D. Flanders, R.L. Carruth, R.M. Izatt and J.J. Christensen, J. Org. Chem., 41 (1976) 134.
[10] G. Wu, W. Jiang, J.D. Lamb, J.S. Bradshaw and R.M. Izatt, J. Am. Chem. Soc., 113 (1991) 6538.
[11] B. de Groot and S.J. Loeb, J. Chem. Soc., Chem. Commun., (1990) 1755.
[12] A.J. Brake, G. Reib and M. Schröder, J. Chem. Soc., Chem. Commun., (1992) 1092.
[13] J.W. Sibert, S.J. Lange, C. Stern, B.M. Hoffman and A.G.M. Barrett, J. Chem. Soc., Chem. Commun., (1994) 1751.
[14] M.G. Banwell, Aust. J. Chem., 44 (1991) 1.
[15] A. Mori, S. Hirayama, Y. Goto and H. Takeshita, Bull. Chem. Soc. Jpn., 61 (1988) 1029.
[16] A. Mori, Y. Isayama, T. Kusaba and H. Takeshita, Eng. Sci. Repts. Kyushu Univ., 6 (1985) 185.
[17] H. Takeshita, A. Mori and S. Hirayama, J. Chem. Soc., Chem. Commun., (1989)564.
[18] S. Hirayama, A. Mori and H. Takeshita, Eng. Sci. Rep. Kyushu Univ., 13 (1992) 349.
[19] H. Takeshita, S. Hirayama and A. Mori, unpublished result.
[20] H. Takeshita, A. Mori and H. Suizu, Chem. Lett., (1986) 593; H. Takeshita, A. Mori and H. Suizu, Bull. Chem. Soc. Jpn., 60 (1987) 1429.
[21] A. Mori, B.-Z. Yin and H. Takeshita, Chem. Express, 7 (1992) 313.
[22] D.E. Bergbreiter and J.R. Blanton, J. Org. Chem., 50 (1985) 5828.
[23] Purchased from Aldrich Co., Ltd., and the acid number was stated as 15 mg KOH/g.
[24] T. Mukai, Bull. Chem. Soc. Jpn., 31 (1958) 846.
[25] H. Takeshita, B.-Z. Yin, K. Kubo and A. Mori, Bull. Chem. Soc. Jpn., 66 (1993) 3451.
[26] H. Takeshita, K. Kubo and A. Mori, unpublished result.
[27] E. Kimura, C.A. Dalimunte, A. Yamashita and R. Machida, J. Chem. Soc., Chem. Commun., (1985) 1041.
[28] H.A. Benesi and J.H. Hildebrand, J. Am. Chem. Soc., 71 (1949) 2703.
[29] R.P. Lange, J. Am. Chem. Soc., 84 (1962) 1185.
[30] Y. Takai, Y. Okumura, T. Tanaka, M. Sawada, S. Takahashi, M. Shiro, M. Kawamura and T. Uchiyama, J. Org. Chem., 59 (1994) 2967; M. Sawada, Y. Okumura, M. Shizuma, T. Takai, Y. Hidaka, H. Yamada, T. Tanaka, T. Kaneda, K. Hirose, S. Misumi and S. Takahashi, J. Am. Chem. Soc., 115 (1993) 7381.
[31] H.-G. Löhr and F. Vögtle, Acc. Chem. Res., 18 (1985) 65.